

Ab Initio Studies of the Radical Cation Diels–Alder Reaction

Udo Haberl,[†] Olaf Wiest,* and Eberhard Steckhan[†]*Contribution from the Department of Chemistry and Biochemistry, University of Notre Dame, Notre Dame, Indiana 46556-5670**Received November 19, 1998. Revised Manuscript Received May 10, 1999*

Abstract: The radical cation Diels–Alder reaction of the 1,3-butadiene radical cation with ethylene, yielding the cyclohexene radical cation, was studied by B3LYP hybrid functional and QCISD(T)//QCISD calculations using the 6-31G* basis set. The intermediates and transition states involved in three different mechanisms, a concerted C_s-symmetric and a stepwise unsymmetric anti [4 + 2] pathway and a stepwise unsymmetric out-gauche pathway leading to vinylcyclobutane, have been considered. The synchronous C_s-symmetric pathway is prevented by a pseudo-Jahn–Teller distortion and is 19 kcal/mol higher in energy than the stepwise pathways. The stepwise anti pathway was found to be the lowest-energy pathway with an activation energy of 0.3 kcal/mol relative to the initially formed ion–molecule complex. The gauche-out pathway, leading to vinylcyclobutane, is 3.5 kcal/mol higher in energy than the anti pathway, leading to cyclohexene. In contrast to earlier calculations by Bauld at the MP2/6-31G*//3-21G level of theory, an ion–molecule complex was found to be part of the reaction pathway and no in-gauche intermediate could be located. The transition structures and intermediates involved in both stepwise pathways closely resemble the previously described species involved in the stepwise mechanism of the neutral Diels–Alder reaction.

Introduction

Among the methods in organic synthesis, the Diels–Alder reaction holds an important position. The [4 + 2] cycloaddition of 1,3 dienes with olefins is one of the most thoroughly studied reactions of organic chemistry. One of the big successes of the Woodward–Hoffmann rules was the mechanistic analysis of this reaction within the molecular orbital theory.¹ Computational chemists have studied the mechanism of the reaction of 1,3 butadiene and ethylene at virtually all feasible levels and have debated whether this prototype Diels–Alder reaction has a concerted pericyclic mechanism or is a stepwise process involving a diradical intermediate.^{2,3} In most neutral [4 + 2] cycloadditions, an electron-rich compound is reacted with an electron-deficient partner to ensure a small HOMO–LUMO gap, which leads to a rapid reaction due to a good interaction of the FMOs. This represents at the same time a synthetic limitation for the Diels–Alder reaction in that reactants with similar electron demand usually react slowly.

The mechanism of the corresponding electron-transfer-catalyzed Diels–Alder reaction, which proceeds via the corresponding radical cations, is much less understood. This lack of basic understanding is unsatisfactory from a scientific point of view and hinders the synthetic application of electron-transfer catalysis. Electron transfer, the most simple method for a redox

umpolung, permits cycloadditions between reactants with similar HOMO energies under mild conditions via electrochemically, photochemically, or chemically generated radical cations. These radical-cation-initiated reactions typically have reaction rates several orders of magnitude greater than the corresponding neutral reactions. Thus, electron-transfer-induced Diels–Alder reactions have proven to be promising tools for organic synthesis⁴ and have been reviewed several times.⁵ The efficient applicability of this reaction to the synthesis of natural products could also be demonstrated.⁶

A common side reaction of the radical cation Diels–Alder reaction is the formation of vinylcyclobutane through a [2 + 2] cycloaddition.⁷ It has been shown that these vinylcyclobutanes can be converted stereospecifically into cyclohexenes through an electron-transfer-catalyzed [1_s,3_r] methylene shift. This “indirect Diels–Alder reaction” has been reported for a number of substrates.⁸

(4) (a) Wiest, O.; Steckhan, E. *Angew. Chem., Int. Ed. Engl.* **1993**, *32*, 901; *Angew. Chem.* **1993**, *105*, 932. (b) Wiest, O.; Steckhan, E. *Tetrahedron Lett.* **1993**, *34*, 6391. (c) Gieseler, A.; Steckhan, E.; Wiest, O.; Knoch, F.; *J. Org. Chem.* **1991**, *56*, 105. (d) Gürtler, C. F.; Steckhan, E.; Blechert, S. *J. Org. Chem.* **1996**, *61*, 4136. (e) Peglow, T.; Blechert, S.; Steckhan, E. *Chem. Eur. J.* **1998**, *4*, 107.

(5) (a) Müller, F.; Mattay, J. *Chem. Rev.* **1993**, *93*, 99. (b) Bauld, N. L. *Tetrahedron* **1989**, *45*, 5307. (c) Chanon, H.; Ebersson, L. *Photoinduced Electron-Transfer Reactions*; Fox, M. A., Chanon, M., Eds.; Elsevier: Amsterdam, The Netherlands, **1988**, p 409. (d) Mattay, J.; Trampe, G.; Runsink, J. *Chem. Ber.* **1988**, *121*, 1991. (e) Bauld, N. L.; Bellville, D. J.; Harirchian, B.; Lorenz, K. T.; Pabon, R. A.; Reynolds, D. W.; Wirth, D. D.; Chiou, H. S.; Marsh, B. K. *Acc. Chem. Res.* **1987**, *20*, 371.

(6) (a) Harirchian, B.; Bauld, N. L. *J. Am. Chem. Soc.* **1989**, *111*, 1826. (b) Gürtler, C. F.; Blechert, S.; Steckhan, E. *Angew. Chem., Intl. Ed. Engl.* **1995**, *34*, 1900.

(7) (a) Pabon, R. A.; Bellville, D. A.; Bauld, N. L. *J. Am. Chem. Soc.* **1984**, *106*, 2730. (b) Reynolds, D. W.; Harirchian, B.; Chiou, H.; Marsh, B. K.; Bauld, N. L. *J. Phys. Org. Chem.* **1989**, *2*, 57.

(8) (a) Botzem, J.; Haberl, U.; Steckhan, E.; Blechert, S. *Acta Chem. Scand.* **1998**, *52*, 175. (b) Pabon, R. A.; Bellville, D. J.; Bauld, N. L. *J. Am. Chem. Soc.* **1984**, *106*, 2730. (c) Bauld, N. L.; Harirchian, B.; Reynolds, D. W.; Whitem J. C. *J. Am. Chem. Soc.* **1988**, *110*, 8111.

[†] Permanent address: Kekulé-Institut für Organische Chemie und Biochemie der Universität Bonn, Gerhard-Domagk-Str. 1, D-53121 Bonn, Germany.

(1) Woodward, R. B.; Hoffmann, R. *Angew. Chem., Int. Ed. Engl.* **1969**, *8*, 781.

(2) For recent reviews, compare: (a) Borden, W. T.; Lonarich, R. J.; Houk, K. N. *Annu. Rev. Phys. Chem.* **1988**, *39*, 213. (b) Sauer, J.; Sustmann, R. *Angew. Chem., Int. Ed. Engl.* **1980**, *19*, 779. (c) Wiest, O.; Montiel, D. C.; Houk, K. N. *J. Phys. Chem. A* **1997**, *101*, 8377. (d) Wiest, O.; Houk, K. N. *Top. Curr. Chem.* **1996**, *183*, 1.

(3) For recent studies, compare, for example: (a) Beno, B. R.; Houk, K. N.; Singleton, D. A. *J. Am. Chem. Soc.* **1997**, *119*, 9984. (b) Karadakov, P. B.; Cooper, D. L.; Gerratt, J. *J. Am. Chem. Soc.* **1998**, *120*, 3975.

The mechanistic aspects of the radical cation Diels–Alder reaction have been investigated in detail, both experimentally and theoretically.⁹ However, no coherent picture of the various possible reaction pathways could be obtained yet. Many of the experimental studies derived from the investigations of the Retro-Diels–Alder reaction of cyclohexenes in the mass spectrometer. Collision-induced decomposition (CID)¹⁰ and CIDNP experiments¹¹ yielded strong evidence for a stepwise mechanism of the reaction through the detection of reaction intermediates. These findings were supported by MINDO/3 and UHF/3-21G calculations that located a “long bond intermediate” of a gauche-in geometry.¹² Subsequent refinements of these calculations using larger basis sets and inclusion of electron correlation by the MP2 and MP3 methods suggested, however, a concerted, nonsynchronous cycloaddition pathway.¹³ Several attempts to develop a qualitative, FMO-based theory of radical ion cycloadditions were not successful, as exemplified by the “role selectivity” model¹⁴ that was disproved experimentally.¹⁵ Nevertheless, relatively simple semiempirical calculations could be used to rationalize the observed regioselectivities of the radical cation cycloadditions.¹⁶

Quantitative MO calculations are powerful tools to elucidate the reaction pathways for these synthetically and mechanistically intriguing processes. An understanding of the transition states and intermediates involved will allow the prediction of selectivities, substituent effects, and stereochemistry of the reaction and broaden the applicability of this powerful method for the catalysis of slow or symmetry-forbidden pericyclic reactions. Recent developments in computational methodology and hardware make the study of the electron-transfer-catalyzed Diels–Alder reaction with the highly correlated ab initio methods possible. This paper presents a high-level theoretical study of the radical cation Diels–Alder reaction using methods that have been demonstrated earlier to give accurate results for the calculation of radical cations and ion–molecule complexes.¹⁷ The intermediates and transition states involved in three different pathways shown in Figure 1 are considered: (i) a concerted C_s -symmetric involving the C_s -symmetric structure $6^{+\bullet}$, (ii) a stepwise unsymmetric anti pathway leading to the cyclohexene radical cation $3^{+\bullet}$ and involving the species $7^{+\bullet}$ – $9^{+\bullet}$, and (iii) a stepwise unsymmetric out-gauche pathway involving the species $10^{+\bullet}$ – $12^{+\bullet}$, leading to the vinylcyclobutane radical cation $14^{+\bullet}$.

Computational Methodology

A suitable treatment of electron correlation is very important for the accurate calculation of radical cations. Our group¹⁸ and others^{17,19} have shown that UHF and UMPn methods are not suitable for the

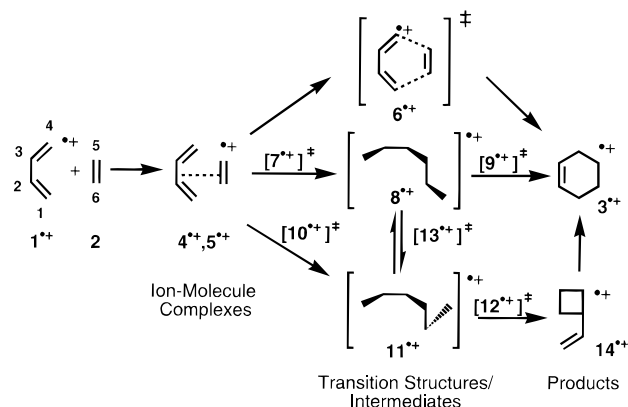


Figure 1. Overview of the species involved in the three pathways for the radical cation Diels–Alder reaction.

calculation of radical ions because the underlying UHF wave function of these species is often severely spin-contaminated. Coupled cluster (CC) and quadratic CI (QCI) methods are less dependent on the quality of the UHF wave function and adequately describe the electron correlation in radical ions and even in systems that are often considered to require multireference treatment.²⁰ In the last five years, hybrid density functional methods such as the B3LYP functional gave results in excellent agreement with the available experimental data and highly correlated MO-based methods.^{21,22} There are, however, recent reports cautioning against the use of the B3LYP and other density functional methods in specialized cases.²³

We therefore adopted a computational strategy in which all structures were fully optimized and characterized at the B3LYP/6-31G* level of theory to ensure that all species have the correct number of negative eigenvalues. The one negative eigenfrequency of the transition structures was animated using MOLDEN²⁴ to ensure that the optimized stationary point corresponds to the transition structure of the desired reaction. This was followed by reoptimization at the QCISD/6-31G* and single-point energy calculations at the QCISD(T)/6-31G* level of theory. In the remainder of the paper, this procedure will be denoted as QCISD(T)//QCISD. All energies reported were corrected for zero-point vibrational energies from B3LYP calculations and are given in kilocalories per mole relative to the cyclohexene radical cation $3^{+\bullet}$ at the same level of theory. All calculations were performed using the G94 series of programs²⁵ running on IBM SP1/SP2 and SGI Origin2000 at the High Performance Computing Complex at the University of Notre Dame.

(18) Wiest, O. *J. Mol. Struct. (THEOCHEM)* **1996**, 368, 39.

(19) (a) Ma, N. L.; Smith, B. J.; Radom, L. *Chem. Phys. Lett.* **1992**, 193, 386. (b) Nobes, R. H.; Moncrieff, D.; Wong, M. W.; Radom, L.; Gill, P. M. W.; Pople, J. A. *Chem. Phys. Lett.* **1991**, 182, 216.

(20) (a) Koga, N.; Morokuma, K. *J. Am. Chem. Soc.* **1991**, 113, 1907. (b) Wierschke, S. G.; Nash, J.; Squires, R. R. *J. Am. Chem. Soc.* **1993**, 115, 11958. (c) Lindh, R.; Perrson, B. J. *J. Am. Chem. Soc.* **1994**, 116, 4963.

(21) (a) Wang, J.; Becke, A. D.; Smith, V. H., Jr. *J. Chem. Phys.* **1995**, 102, 3477. (b) Lamington, G. J.; Handy, N.; Amos, R. D. *Mol. Phys.* **1993**, 80, 1121.

(22) (a) Clark, T. *Top. Curr. Chem.* **1996**, 177, 1. (b) Murray, C. W.; Handy, N. C.; *J. Chem. Phys.* **1992**, 97, 6509. (c) Handy, N. C.; Ma, N. L.; Smith, B. J.; Pople, J. A.; Radom, L. *J. Am. Chem. Soc.* **1991**, 113, 7903.

(23) (a) Bally, T.; Sastry, G. N. *J. Phys. Chem. A* **1997**, 101, 7923. (b) Braida, B.; Hiberty, P. C.; Savin, A. *J. Phys. Chem. A* **1998**, 102, 7872. (c) Sodupe, N.; Bertran, J.; Rodriguez-Santiago, L.; Baerenz, E. J. *J. Phys. Chem. A* **1999**, 103, 166.

(24) MOLDEN Version 3.2 written by G. Schaftenaar (Netherlands). For details of this program, see the URL: <http://www.caos.kun.nl/~schaft/molden>.

(25) Frisch, M. J.; Trucks, G. W.; Schlegel, H. B.; Gill, P. M. W.; Johnson, B. G.; Robb, M. A.; Cheeseman, J. R.; Keith, T.; Petersson, G. A.; Montgomery, J. A.; Raghavachari, K.; I-Laham, M. A.; Zakrzewski, V. G.; Ortiz, J. V.; Foresman, J. B.; Peng, C. Y.; Ayala, P. Y.; Chen, W.; Wong, M. W.; Andres, J. L.; Replogle, E. S.; Gomperts, R.; Martin, R. L.; Fox, D. J.; Binkley, J. S.; Defrees, D. J.; Baker, J.; Stewart, J. P.; Head-Gordon, M.; Gonzalez, C.; Pople, J. A. *Gaussian 94*; Gaussian, Inc.: Pittsburgh, PA, 1995.

(9) (a) Lorenz, K. T.; Bauld, N. L. *J. Am. Chem. Soc.* **1987**, 109, 1157. (b) Reynolds, D. W.; Lorenz, K. T.; Chiou, H. S.; Bellville, D. J.; Pabon, R. A.; Bauld, N. L. *J. Am. Chem. Soc.* **1987**, 109, 4960. (c) Gassmann, P. G.; Singleton, D. A. *J. Am. Chem. Soc.* **1984**, 106, 7993.

(10) Turecek, F.; Hanus, V. *Mass Spectrom. Rev.* **1984**, 3, 85.

(11) (a) Roth, H. D.; Schilling, M. L. M.; Abelt, C. L. *Tetrahedron* **1986**, 42, 6157. (b) Roth, H. D.; Schilling, M. L. *J. Am. Chem. Soc.* **1985**, 107, 716.

(12) Bellville, D. J.; Bauld, N. L. *Tetrahedron* **1986**, 42, 6167.

(13) (a) Bauld, N. L.; Bellville, D. J.; Pabon, R. A.; Chelsky, R.; Green, G. J. *J. Am. Chem. Soc.* **1983**, 105, 2378. (b) Bellville, D. J.; Bauld, N. L.; Pabon, R. A.; Gardner, S. A. *J. Am. Chem. Soc.* **1983**, 105, 3584. (c) Bauld, N. L. *J. Am. Chem. Soc.* **1992**, 114, 5800.

(14) Bellville, D. J.; Bauld, N. L. *J. Am. Chem. Soc.* **1982**, 104, 2665.

(15) Mlcoch, J.; Steckhan, E. *Tetrahedron Lett.* **1987**, 27, 1081.

(16) Wiest, O.; Steckhan, E.; Grein, F. *J. Org. Chem.* **1992**, 57, 4034.

(17) (a) Hrouda, V.; Carsky, P.; Ingr, M.; Chval, Z.; Sastry, G. N.; Bally, T. *J. Phys. Chem. A* **1998**, 102, 9297. (b) Hrouda, V.; Roeselova, M.; Bally, T. *J. Phys. Chem. A* **1997**, 101, 3925. (c) Jungwirth, P.; Bally, T. *J. Am. Chem. Soc.* **1993**, 115, 5783.

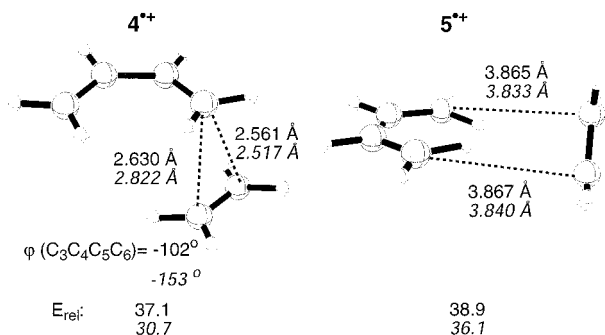


Figure 2. Ion–molecule complexes 4^{+} and 5^{+} of the butadiene radical cation with ethylene. Results from QCISD(T)/QCISD calculations are in plain text, and results from B3LYP calculations are in italics.

Results

Ion–Molecule Complexes. In the gas phase, the interaction between a charged species and an olefin leads to the formation of ion–molecule complexes. As a first step in the investigation of the reaction of the butadiene radical cation 1^{+} with ethylene **2**, the interactions of the reactants were examined. Several starting geometries with different relative orientations of 1^{+} and **2** were chosen for the geometry optimizations. All calculations converged to either of the two ion–molecule complexes 4^{+} and 5^{+} shown in Figure 2. A normal-mode analysis confirmed the structures as local energy minima on the $C_6H_{10}^{+}$ hypersurface. The attempted optimization of a C_s -symmetric ion–molecule complex did not lead to a minimum on the hypersurface.

The ion–molecule complex 4^{+} is the first step of the addition of a butadiene radical cation to ethylene. The binding energy in this complex is 11.0 kcal/mol at the B3LYP level and 7.6 kcal/mol at the QCISD(T)/QCISD level relative to the isolated starting compounds 1^{+} and **2**.²⁶ The smallest atomic distances between the two moieties of 4^{+} are the carbon–carbon distances $R_{4,5} = 2.52$ Å and $R_{4,6} = 2.82$ Å. The fact that these distances are rather large and that there is little pyramidalization in the butadiene and the ethylene moieties leads to the conclusion that there are no significant covalent interactions between the moieties. The approach via the intermediate 4^{+} leads to the stepwise anti or the out-gauche pathway described below.

The second ion–molecule complex 5^{+} represents a C_2 -symmetric antarafacial/suprafacial approach of ethylene to the butadiene radical cation and is 5.4 kcal/mol higher in energy than the ion–molecule complex 4^{+} . The closest distance between the carbon atoms of ethylene and the hydrogen atoms of the butadiene radical cation is 2.98 Å. The dihedral angle between the central C_2 – C_3 bond of the butadiene moiety C_5 – C_6 in the ethylene part is -118 degrees; that is, the butadiene and ethylene moieties are almost perpendicular to each other as can be seen in Figure 2. This indicates an even weaker interaction between the fragments than in the ion–molecule complex discussed above. We have not been able to locate a reactive pathway leading from 5^{+} to any of the intermediates discussed below. Therefore and because of the substantial energy differences of 1.7 and 5.4 kcal/mol at the QCISD(T)/QCISD and the B3LYP levels, respectively, we conclude that 5^{+} is not likely to be involved in the reaction pathway.

(26) The basis set superposition error in the calculation of the interaction energy in the ion–molecule complexes 4^{+} and 5^{+} at the B3LYP level is small. An estimate of the BSSE by a counterpoise calculation gave corrections of 0.47 and 0.12 kcal/mol, respectively. At the QCISD(T)/QCISD level, the BSSE is with 2.44 and 7.46 kcal/mol higher.

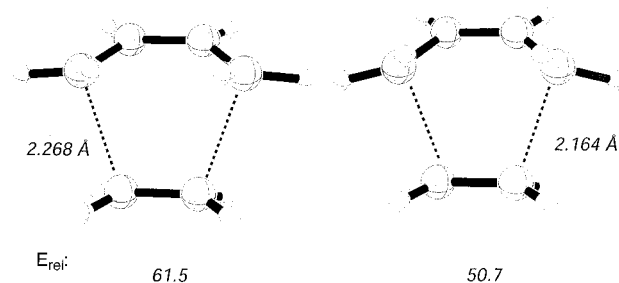


Figure 3. B3LYP transition structure **6** (left) and second-order saddle point 6^{+} of the synchronous, C_s -symmetric pathway of the neutral and radical cation Diels–Alder reaction.

The Synchronous Pathway. The concerted, C_s -symmetrical pathway has been investigated for a comparison with the stepwise unsymmetrical reaction paths. The stationary point 6^{+} obtained at the B3LYP level of theory is shown on the right in Figure 3 together with selected geometric parameters. The geometry is very similar to the well-known C_s -symmetric transition structure for the neutral Diels–Alder reaction of butadiene with ethylene, shown on the left of Figure 3.²⁷ The carbon–carbon bond distance computed for the breaking bond is 2.16 Å and is 0.1 Å shorter than the one calculated for the neutral reaction, which is 2.27 Å. The reason for this contraction is a charge-transfer interaction in 6^{+} where 0.32 electrons are transferred from the olefin to the diene radical cation. This interaction is not present in the neutral transition state.

The energy of 6^{+} relative to the cyclohexene radical cation 3^{+} is 10.8 kcal/mol lower than the corresponding energy of transition state **6** in the C_s -symmetric, synchronous pathway relative to **3**. Although these results appear to be reasonable, the frequency analysis of 6^{+} at the B3LYP level of theory reveals that this stationary point is a second-order saddle point and therefore not a true transition structure. The first imaginary frequency of -1030 cm^{-1} is unusually strong and corresponds to the antisymmetric motion of the butadiene carbons. This symmetry-breaking mode is caused by a pseudo-Jahn–Teller distortion of the C_s -symmetric transition structure 6^{+} and leads to a stabilization of a dissymmetric structure and disfavors the C_s -symmetric pathway. Similar results have been obtained earlier for the ring-opening reactions of the cyclobutene radical cation²⁸ and the cyclopropane radical cation.²⁹ The activation barrier of the synchronous pathway is 19 kcal/mol higher in energy than the stepwise, unsymmetrical pathway described below. The synchronous pathway is therefore strongly disfavored and was not further considered.

The Anti Pathway. If the C_4 – C_5 distance in the ion–molecule complex 4^{+} is decreased, the first-order saddle point 7^{+} shown in Figure 4 is obtained. 7^{+} is a true transition structure with one imaginary frequency corresponding to a bond-breaking mode of the carbons C_4 and C_5 . The distance of these atoms is 2.15 Å in the transition structure. The activation energy of the step from the ion–molecule complex 4^{+} to the transition structure 7^{+} is only 0.3 and 0.5 kcal/mol at the QCISD(T)/QCISD and B3LYP levels of theory, respectively. The finding that 7^{+} connects the ion–molecule complex 4^{+} to the pathway that leads ultimately to the products of the reaction is in contrast with earlier calculations which gave no evidence for the involvement of the ion–molecule complexes in the reaction

(27) Goldstein, E.; Beno, B.; Houk, K. N. *J. Am. Chem. Soc.* **1996**, *118*, 6036.

(28) (a) Wiest, O. *J. Am. Chem. Soc.* **1997**, *119*, 5713. (b) Sastry G. N.; Bally, T.; Hrouda, V.; Carsky, P. *J. Am. Chem. Soc.* **1998**, *120*, 9323.

(29) Bischoff, P. J. *J. Am. Chem. Soc.* **1977**, *99*, 8145.

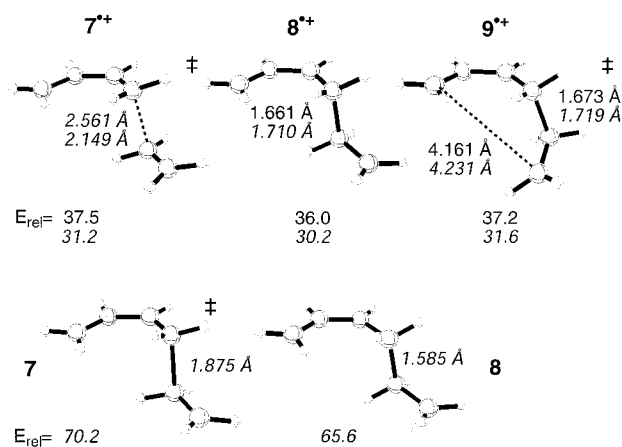


Figure 4. (Top) Transition structures 7^{*+} and 9^{*+} and intermediate 8^{*+} for the anti pathway. Results from QCISD(T)/QCISD calculations are in plain text, and results from B3LYP calculations are in italics. (Bottom) B3LYP/6-31G* transition structure **7** and intermediate **8** for the anti pathway of the neutral, stepwise Diels–Alder reaction (from ref 27).

pathway.^{13c} The activation barriers calculated by the different methods for this stepwise pathway are consistently lower by 19.5 kcal/mol as compared with the synchronous, C_5 -symmetrical pathway via the transition state 6^{*+} . It is evident that the two stepwise, unsymmetrical pathways are energetically favored over the synchronous process.

The transition vector in 7^{*+} leads to the formation of a carbon–carbon bond and to the intermediate 8^{*+} as a local minimum on the potential hypersurface. This intermediate has an anti conformation with respect to the torsion C_3 – C_4 – C_5 – C_6 of the newly formed bond and has a bond distance C_4 – C_5 of 1.71 Å. An analysis of the charge and spin distribution in 8^{*+} indicates a positive charge of 0.53 in the allyl moiety and a spin density of 0.71 at C_6 . In this structure, the positive charge is localized as an allyl cation on C_1 – C_3 and the spin density is localized predominantly as a methylene radical at C_6 . There is good agreement between the results from the B3LYP calculations and the QCISD(T)/QCISD reference calculations that increase our confidence in the applicability of the B3LYP method to the radical cation Diels–Alder reaction. 8^{*+} connects to the cyclohexene radical cation 3^{*+} via the transition structure 9^{*+} . The gauche-in structure of the long bond intermediate described previously at the MP2/6-31G**/3-21G level of theory^{13c} for this reaction is therefore not part of the pathway at higher levels of theory. Instead, the intermediate detected by CIDNP and CID studies^{10,11} is more likely to correspond to the intermediate 8^{*+} . At the QCISD(T)/QCISD level of theory, transition structure 9^{*+} is only 1.2 kcal/mol higher in energy than the intermediate 8^{*+} . The transition vector in 9^{*+} has a low frequency of -85 cm^{-1} that corresponds to the rotation around the C_4 – C_5 single bond. IRC calculations at the B3LYP level of theory indicate that there is no further intermediate involved in the ring closure. This is similar to earlier findings by Bauld, who showed that the gauche-in intermediate located by UHF calculations is not a stationary point at theory levels that consider electron correlation.^{13c} At the same time, the presence of 8^{*+} as an intermediate at both levels of theory used here is in contradiction to Bauld's calculations, which predicted a concerted reaction mechanism.

The structures 7^{*+} and 8^{*+} strongly resemble the transition structures and intermediates **7** and **8** located at the B3LYP/6-31G* level of theory by Goldstein et al. for the stepwise, diradical mechanism of the neutral Diels–Alder reaction.²⁷

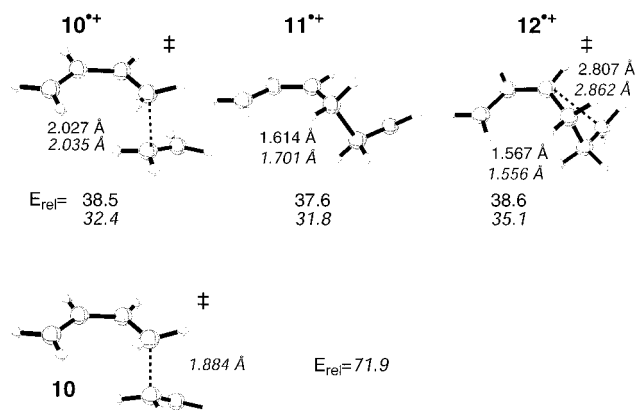


Figure 5. (Top) Transition structures 10^{*+} and 12^{*+} and intermediate 11^{*+} for the out-gauche pathway. Results from QCISD(T)/QCISD calculations are in plain text, and results from B3LYP calculations are in italics. (Bottom) B3LYP/6-31G* transition structure **10** for the out-gauche pathway of the neutral, stepwise Diels–Alder reaction (from ref 27).

These structures and their energies (relative to cyclohexene) are shown for comparison in the lower panel of Figure 4. In agreement with the localization of the HOMO in the C_4 – C_5 bond of **8** and the relative thermochemistry for the formation of **8** and 8^{*+} , the C_4 – C_5 bond in 7^{*+} is 0.27 Å longer than in **7** and 0.125 Å longer in 8^{*+} than in **8**. So far, no transition structure or intermediate corresponding to a putative gauche-in biradical **9** could be located.³⁰

The Out-Gauche Pathway. An additional first-order saddle point was found with an out-gauche conformation with respect to the torsion angle C_3 – C_4 – C_5 – C_6 . This transition structure 10^{*+} is shown in Figure 5 on the left. The activation barrier of the step from the ion–molecule complex 4^{*+} to this transition structure at the QCISD(T)/QCISD level is 1.0 and 1.2 kcal/mol at the B3LYP level higher than the activation barrier leading to the anti transition structure 7^{*+} . The imaginary frequency of 10^{*+} corresponds to a bond-breaking mode of the carbons C_4 and C_5 , with a distance of 2.03 Å between these atoms.

This normal mode associated with the imaginary frequency of the transition structure 10^{*+} leads to the formation of a carbon–carbon bond in the intermediate 11^{*+} , also shown in Figure 5. Similar to the anti intermediate 8^{*+} , 11^{*+} has the localized character of a primary methylene radical and an allyl cation. The C_4 – C_5 bond is already fully formed with calculated bond lengths of 1.614 and 1.701 Å at the QCISD and B3LYP levels of theory, respectively. At both levels of theory, the out-gauche intermediate is 1.6 kcal/mol higher in energy than the corresponding anti intermediate 8^{*+} . Only the first transition structure of the out-gauche pathway of the stepwise neutral Diels–Alder reaction, **10**, has been reported and is shown for comparison in the lower part of Figure 5.²⁷ 10^{*+} again resembles that transition structure. This is in analogy to the anti pathway described above, indicating that the similarities between the structures involved in the neutral, diradical, and the radical cationic pathways may have some generality.

Ring closure of the 11^{*+} to form the product of the reaction, the vinylcyclobutane radical cation 14^{*+} , proceeds via transition structure 12^{*+} , shown in Figure 5 on the right. It is noteworthy that at the QCISD level of theory, the methylene group at C_6 is with a dihedral angle C_4 – C_5 – C_6 –H of 44.4° considerably rotated from its original position perpendicular to the forming

(30) Beno, B.; Wilsey, S.; Houk, K. N. *J. Am. Chem. Soc.* **1999**, *121*, 4816.

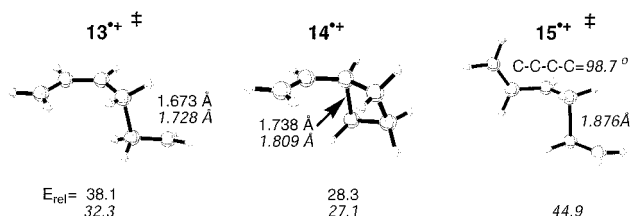


Figure 6. Transition structure 13^{*+} for the interconversion of 8^{*+} and 11^{*+} (left), vinylcyclobutane radical cation 14^{*+} (middle), and transition structure 15^{*+} for the cis/trans isomerization of the C_2-C_3 bond in 8^{*+} . Results from QCISD(T)//QCISD calculations are in plain text, and results from B3LYP calculations are in italics.

C_4-C_5 bond. Although this is in agreement with the suprafacial stereochemistry predicted for [2 + 2] cycloadditions by simple orbital symmetry considerations, it should be pointed out that these rules are usually not applicable because it is not clear which of the three possible interactions between HOMO, SOMO, and LUMO is the dominant one.³¹ Closer analysis of the molecular orbitals reveals that this orientation of the methylene group is necessary to achieve a binding interaction between the SOMO, centered at C_6 , with the LUMO at C_3 . In this conformation, however, the binding interaction between the SOMO and the HOMO, centered on the newly formed C_4-C_5 bond, is disrupted. This destabilizes 12^{*+} , making it 3.3 and 1 kcal/mol less stable to 11^{*+} at the B3LYP and QCISD(T)/QCISD levels of theory, respectively. At these two levels of theory, this pathway is 3.5 and 1.1 kcal/mol less favorable than the competing formation of 3^{*+} . In agreement with the experimental findings, this energy difference is large enough to prevent the formation of larger quantities of the [2 + 2] cycloadduct 14^{*+} under normal conditions. The absolute energy difference is, however, very small and could easily be overcome through steric or electronic factors of substituents.

The out-gauche intermediate 11^{*+} can also be formed from the anti intermediate 8^{*+} by rotation around the C_4-C_5 bond. The transition structure for this rotation, 13^{*+} , is shown in Figure 6 on the left. 13^{*+} is structurally quite similar to 9^{*+} except for the dihedral angle around the C_4-C_5 bond which is 113.4 degrees in 13^{*+} as compared to -122.9 degrees in 9^{*+} . With an energy of 2.1 kcal/mol higher than 8^{*+} , this pathway is disfavored relative to the ring closure to 3^{*+} , but the differences are again small enough to be reversed by minor changes in substitution patterns.

The product of the [2 + 2] cycloaddition, the vinylcyclobutane radical cation 14^{*+} , is shown in the middle of Figure 6. Vinylcyclobutanes have been observed experimentally as the products of the electron-transfer-catalyzed reaction of dienes and olefins in a number of cases.^{7,8} Even though 14^{*+} is 28.3 kcal/mol less stable than 3^{*+} at the QCISD(T) level of theory, it can be the exclusive product of the reaction, for example, when the diene radical cation is in the s-trans conformation. In this case, only the [2 + 2] cycloaddition to 14^{*+} is possible, but not a [4 + 2] cycloaddition. For the parent reaction, no isomerization on the stage on the intermediate is possible because this would require the rotation around the allylic C_2-C_3 bond. The B3LYP transition structure for this rotation derived for the intermediate of the anti pathway, 15^{*+} , is shown in Figure 6 on the right. At this level of theory, it is 14.7 kcal/mol higher in energy than 8^{*+} . The reaction of s-trans butadiene followed by rotation around the C_2-C_3 bond is therefore not competitive

(31) It has for, example, been shown that the [2 + 2] cycloreversion of the cyclobutane radical cation proceeds in a supra-suprafacial manner (compare ref 17c).

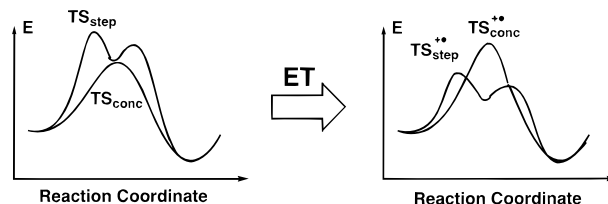


Figure 7. Schematic representation of the effect of electron transfer on a pericyclic reaction.

with the ring closure to 14^{*+} . The cis–trans isomerization of the C_2-C_3 bond may, however, be possible in substituted cases where the allylic character of this bond is diminished.^{8a} Alternative pathways from predominantly s-trans dienes to cyclohexenes include the formation of 14^{*+} , which can then rearrange to 3^{*+} , or the easy rotation around a single bond in 14^{*+} described by Hofmann and Schaefer and discussed below. It was shown experimentally that 14 can be converted to 3 under electron-transfer conditions in a stereospecific manner. Our study demonstrates that the mechanisms of the radical cation Diels–Alder reaction and the vinylcyclobutane rearrangement cannot be separated into two different mechanisms. Both reactions take place at the same potential-energy hypersurface.

Conclusions

For the two energetically viable pathways, the anti pathway and the out-gauche pathway, there is a striking resemblance between the structures calculated for the radical cation and the stepwise biradical pathways. These similarities can be rationalized by considering the effects of an electron transfer onto a pericyclic reaction as shown schematically in Figure 7. In a typical pericyclic reaction, the low-energy pathway goes through an aromatic-type transition structure TS_{conc} . The corresponding stepwise pathway is disfavored by the “energy of concert” due to the energy required for the bond homolysis in TS_{step} , inducing the reaction. As shown on the right in Figure 7, electron transfer disfavors the concerted pathway because the corresponding transition state TS_{conc}^{*+} does not benefit from aromatic stabilization. The stepwise pathway is on the other hand promoted because the homolysis of a one-electron bond is facile. If the energy of concert for a reaction is small, an electron transfer will therefore lead to a stepwise pathway. The transition states TS_{step} and the intermediates of the neutral and the radical cationic pathway should then be related to each other in a predictable fashion. Should such a relationship be shown to be more general, it could increase our understanding of electron-transfer-catalyzed reactions by providing a link between pericyclic reactions of radical cations and the much better understood stepwise pathways of pericyclic reactions. Experimental support for this hypothesis comes also from the detection of the cyclohexane-1,4-diyl radical cation intermediate by ESR after one-electron oxidation of 1,5 hexadiene.³² This intermediate can be viewed as the equivalent of the postulated cyclohexane-1,4-diyl frequently postulated as an intermediate in the Cope rearrangement.³³ Nevertheless, further work on other reactions will be necessary to investigate the applicability of this argument.

Another feature the radical cation Diels–Alder reaction shares with many biradical³⁴ and ion–molecule reactions¹⁷ is the

(32) Williams, F. *J. Chem. Soc., Faraday Trans.* **1994**, *90*, 1681.

(33) (a) Osamura, K.; Kato, S.; Morokuma, K.; Feller, D.; Davidson, E. R.; Borden, W. T. *J. Am. Chem. Soc.* **1984**, *106*, 3362. (b) Dupuis, M.; Murray, C.; Davidson, E. R. *J. Am. Chem. Soc.* **1991**, *113*, 9756.

(34) For recent examples, compare, for example: (a) Doubleday, C.; Bolton, K.; Hase, W. L. *J. Phys. Chem. A* **1998**, *102*, 3648. (b) Carpenter, B. K. *J. Am. Chem. Soc.* **1995**, *117*, 6336. (c) Carpenter, B. K. *Am. Sci.* **1997**, *85*, 138.

extraordinary flatness of the potential-energy surface. At the highest level of theory used here, the ion–molecule complexes 4^{+} and 5^{+} as well as the transition structures and reactive intermediates 7^{+} to 13^{+} are within an energy range of less than 5 kcal/mol. It is also possible that there are other stationary points of similar energy which are not described here. It can therefore be expected that in analogy to biradical type reactions,³⁴ dynamic factors will be important for the reaction outcome in some cases.

Our results also show that the products of the [4 + 2] cycloaddition, 3^{+} , and the [2 + 2] cycloaddition, 14^{+} , are derived from the same reaction pathway. The two products can be derived either from the common ion–molecule complex 4^{+} via the out-gauche intermediate 11^{+} or by counterclockwise rotation around the C₄–C₅ bond in the anti intermediate 8^{+} . Similar conclusions have been drawn for the [2 + 2] and [4 + 2] cycloaddition of butadiene and 1,1-dichloro-2,2-difluoroethene, which is thought to proceed via a stepwise pathway and has identical activation energies and volumes for the formation of the cyclohexene and vinylcyclobutane products.³⁵ This indicates that the rate-determining transition states for the formation of the two products are very similar.

The thermochemistry of the overall reaction of 1^{+} and **2** to form 3^{+} computed by the two methods used here is in very good agreement with the value of 42.5 ± 0.8 deduced from experimental data.³⁶ The QCISD(T)/QCISD calculations slightly overestimate the heat of reaction with a computed value of 44.8 kcal/mol, whereas the value of 41.8 kcal/mol calculated at the B3LYP level of theory is within experimental error. Finally, we note that the relative energies for all reactive intermediates and transition structures obtained by the B3LYP calculations are in excellent agreement with those from the QCISD(T)/QCISD reference calculations. The energies relative to 3^{+} are, however, consistently lower by 6 kcal/mol due to the larger exothermicity of the reaction at the QCISD(T)/QCISD level. An analysis of the electronic structure of the species involved shows that this is not due to the previously described overestimation of delocalization.²² Instead, the electronic structure of the intermediates 8^{+} and 11^{+} can be best described as a methylene radical connected to an allyl cation. The inability of the B3LYP method to yield localized structures in the butadiene radical cation does not appear to be a problem in these less-conjugated structures. It can therefore be concluded that the B3LYP method is an efficient tool for the study of potentially much larger and chemically more realistic systems.

Summary and Outlook

QCISD(T)/QCISD and hybrid DFT calculations show that the lowest-energy pathway for the reaction of ethylene **2** with the butadiene radical cation 1^{+} is the [4 + 2] cycloaddition to form the cyclohexene radical cation 3^{+} . The barrier for the

formation of the [2 + 2] adduct is 3.5 kcal/mol higher. The two pathways start from a common ion–molecule complex and interconnect through a transition structure 13^{+} that converts the intermediates of the two pathways into each other. The symmetric, C_s-symmetrical pathway is strongly disfavored through a second-order Jahn–Teller distortion. The calculated structures strongly resemble the ones described earlier for the diradical, stepwise pathway of the neutral Diels–Alder reaction. This is rationalized in terms of the effect of an electron transfer on the competing concerted and stepwise processes.

Future studies will test the generality of the proposed similarity between the radical cationic and the stepwise, diradical pathways of pericyclic reactions, which could potentially be used as a predictive model for a rational design of electron-transfer-catalyzed reactions. The excellent agreement of the results from the computationally efficient B3LYP method with the data obtained from the QCISD(T)/QCISD reference calculations also encourages the investigation of larger, chemically more relevant systems. These studies are currently in process and will be reported elsewhere.³⁷

Comparison with the Results of Hofmann and Schaefer.

After the completion of this study, we learned of a related study by Hofmann and Schaefer.³⁸ This study provides a more comprehensive view of the C₆H₁₀^{•+} hypersurface, including several pathways not included in our study. Here, the easy cis/trans isomerization of the *trans*-1,3-butadiene radical cation via the vinylcyclobutane radical cation and the formation of methylcyclopentene, which was to the best of our knowledge never observed experimentally, are particularly interesting. There are also some smaller differences in the pathways computed in both studies, namely the stepwise [3 + 2] cycloaddition to form cyclohexene and the [2 + 1] cycloaddition of the *cis*-1,3-butadiene radical cation and ethylene. Here, several additional stationary points, usually in very shallow wells on the hypersurface, have been located by Hofmann and Schaefer. Several of the differences between the pathways obtained by the two studies are likely to be the results of the different methods used. As discussed earlier, the UMP2 method has been shown to give unreliable energies for highly spin-contaminated species such as the structures **2**, **3**, and **8** or most of the transition structures described in the study by Hofmann and Schaefer. This is due to a bias of the UMP2 methods toward structures that localize spin and charge. On very flat potential-energy hypersurfaces such as the C₆H₁₀^{•+} hypersurface, this is likely to have a large effect on the structure and characteristics of the stationary points on the hypersurface. A similar situation was obtained in the case of the ring opening of the cyclobutene radical cation, where QCISD(T)/6-31G*//QCISD/6-31G* calculations located a relatively small number of stationary points. In contrast, UMP2 calculations gave a large number of stationary points on the so-called “Bauld Plateau” that disappeared upon reoptimization with highly correlated methods. It therefore seems that several, if not all, of these additional stationary points on the hypersurface are artifacts of the application of the UMP2 method to highly spin-contaminated wave functions.³⁹ It should, however, be pointed out that these minima have only a small chemical

(35) (a) Swenton, J. S.; Bartlett, P. D. *J. Am. Chem. Soc.* **1968**, *90*, 2056. (b) Klärner, F.-G.; Krawczyk, B.; Ruster, V.; Deiters, U. K. *J. Am. Chem. Soc.* **1994**, *116*, 7646.

(36) Calculated from $\Delta H_f^\circ(1,3\text{-butadiene}) = 26.0 \pm 0.19$ kcal/mol, IE (1,3-butadiene) = 9.072 ± 0.007 eV, $\Delta H_f^\circ(\text{ethylene}) = 12.5399 \pm 0.0006$ kcal/mol, $\Delta H_f^\circ(\text{cyclohexene}) = -1.03 \pm 0.23$ kcal/mol, IE (cyclohexene) = 8.945 ± 0.010 eV. (a) Prosen, E. J.; Maron, F. W.; Rossini, F. D. *J. Res. Natl. Bur. Stand. (U.S.)* **1951**, *46*, 106. (b) Chase, M. W., Jr. *J. Phys. Chem. Ref. Data, Monograph 9*, **1998**, 1. (c) Steele, W. V.; Chirico, R. D.; Knipmeyer, S. E.; Nguyen, A.; Smith, N. K.; Tasker, I. R. *J. Chem. Eng. Data*, **1996**, *41*, 1269. (d) Lias, S. D.; Bartmess, J. E.; Liebman, J. F.; Holmes, J. L.; Levin, R. D.; Mallard, W. G. Ion Energetics Data. In *NIST Chemistry WebBook*; Mallard, W. G., Linstrom, P. J., Eds.; NIST Standard Reference Database Number 69, November 1998, National Institute of Standards and Technology, Gaithersburg MD, 20899 (<http://webbook.nist.gov>).

(37) Haberl, U.; Steckhan, E.; Blechert, S.; Wiest, O. *Chem. Eur. J.*, in press.

(38) Hofmann, M.; Schaefer, H. F., III *J. Am. Chem. Soc.* **1999**, *121*, 6719–6729. Our 1^{+} corresponds to Hoffman and Schaefer's **2**, **2** to **1**, 4^{+} to **3**, 7^{+} to **TS-3/4**, 8^{+} to **9**, 11^{+} to **4**, 12^{+} to **TS-4/10**, and 14^{+} to **10**.

(39) For a detailed discussion, compare: Bally, T.; Borden, W. T. In *Reviews in Computational Chemistry*; Lipkowitz, K. B., Boyd, D. B., Eds.; VCH–Wiley: New York, 1999; Vol. 13.

significance because they are in very shallow grooves of the potential-energy hypersurface. Moreover, it has been shown for the case of the cyclobutene radical cation ring opening that any preferences can be easily overcome by solvent⁴⁰ or substituent effects.⁴¹ Finally, the excellent agreement between the B3LYP and the QCISD(T)/QCISD reference calculations demonstrates that the problem of “inverse symmetry breaking”³⁸ described earlier is not an issue for the reaction studied here. It appears that this problem occurs only in symmetric structures, even though the theoretical analysis should apply to symmetric and dissymmetric structures alike. Future theoretical work will be necessary to determine whether the findings described here are generally true for dissymmetric structures.

(40) Barone, V.; Rega, N.; Bally, T. *J. Phys. Chem A* **1999**, *103*, 217.

(41) Swinarski, D. J.; Wiest, O., to be submitted for publication.

Acknowledgment. We are grateful to the Office of Information Technologies at the University of Notre Dame and the National Center for Supercomputer Applications (NCSA) for generous allocation of computing resources. Financial support provided by the Volkswagen Stiftung (Grants I/72 647 to O.W. and I/71 748 to E.S.), the National Science Foundation (Grant CHE-9733050 to O.W.), and the Fonds der Chemischen Industrie (E.S.) is gratefully acknowledged. We would also like to thank Dr. Hofmann for a preprint of ref 38.

Supporting Information Available: Energies, zero-point energies, imaginary frequencies, and Cartesian coordinates of all structures reported in ASCII format. This material is available free of charge via the Internet at <http://pubs.acs.org>.

JA983993Y